

Relative Signs of NMR Spin Coupling Constants by Two-Dimensional Fourier Transform Spectroscopy

AD BAX

Department of Applied Physics, Delft University of Technology, Delft, The Netherlands

AND

RAY FREEMAN

Physical Chemistry Laboratory, Oxford University, Oxford OX1 302, England

Received June 22, 1981

Conventional high-resolution NMR spectra yield the magnitudes of the spin coupling constants but not their signs. When relative sign information is required it is necessary to set up a further experiment employing selective double resonance (1-3) or proceed to a detailed analysis of a strongly coupled spectrum (4). In certain circumstances, relative sign information can be used as a diagnostic tool, for example, in the recognition of geminal and vicinal proton-proton couplings, which normally have opposite signs. The present work describes a simple two-dimensional Fourier transform experiment (5, 6) in which relative signs of coupling constants are obtained directly by inspection (7).

The basic requirement for any relative sign determination is a system of three coupled nonequivalent spins, for example, an AMX system. It is useful for this discussion to introduce the concept of a "passive" spin, say, the M spin in this case. The role of the M spin is limited to the creation of two AX subspectra, one corresponding to M in an α spin state, the other to M in a β spin state. Apart from introducing the two couplings J_{AM} and J_{MX} , the passive spin M is not involved and its resonance need not be observed. Double resonance provides a method for recognizing which A and X lines belong to a given AX subspectrum, and it is well known that if the upfield A doublet is associated with the upfield X doublet, then J_{AM} and J_{MX} have like signs (1-3).

A new approach to relative sign determination is provided by magnetization transfer experiments studied by two-dimensional Fourier transformation (5, 6). The magnetization of the A spin is labeled in terms of the characteristic precession frequencies by allowing transverse A-magnetization to evolve during a variable interval t_1 . A second pulse (known as a "mixing pulse") converts this back into Z magnetization, equivalent to a disturbance of the energy level populations. These population changes affect the intensities of the X signals when the

converted to a spectrum $S(F_1, F_2)$ by two-dimensional Fourier transformation (8-10). For this simple AX case the spectrum consists of just four lines in a square pattern. The center of the square has the coordinates δ_A, δ_X and the sides are J_{AX} Hz in length.

The introduction of a third spin M splits this two-dimensional spectrum into subspectra. In the general case the mixing pulse transfers magnetization from all A transitions to all X transitions, giving rise to *four* subspectra, but if the mixing pulse has only a small flip angle (6, 11) then M remains truly "passive" and does not change its spin state when magnetization is transferred from A to X. The transfer is then selective and there are only *two* subspectra of appreciable intensity, giving rise to two square patterns of four lines each. The displacement of one such square with respect to the other reflects the influence of the M spin.

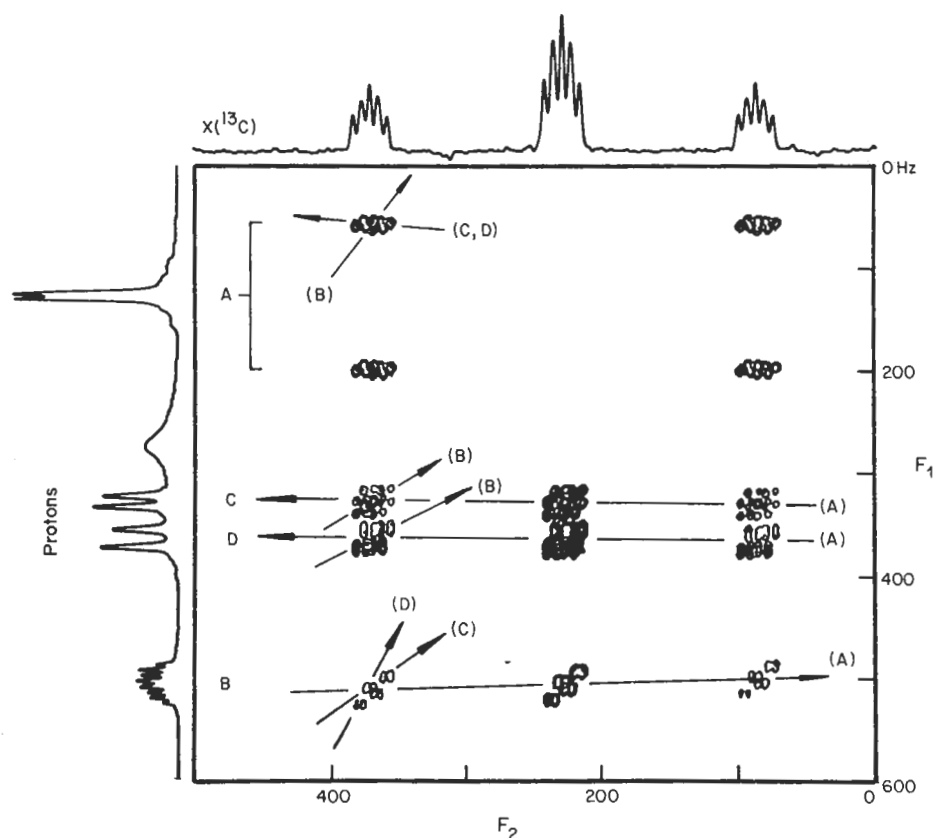


FIG. 2. Two-dimensional spectrum of allyl alcohol obtained by transferring magnetization from protons to the methylene carbon site. The conventional proton spectrum is shown in the left-hand margin and the carbon-13 multiplet is shown at the top of the diagram. The various tilts within a given two-dimensional multiplet are indicated by the arrows, labeled according to the "passive" spins associated with that particular transfer (in parentheses). The coupling J_{CD} is too small to produce a detectable tilt, and at the top left of the diagram the tilt due to the small couplings J_{AC} and J_{AD} is only apparent because they have a cumulative effect.

When this displacement is in the same sense along F_1 and F_2 , then J_{AM} and J_{MX} have like signs. A line joining the centers of the two squares has a positive slope for like signs and a negative slope for opposite signs. A zero or infinite slope indicates that either J_{AM} or J_{MX} is vanishingly small. The analogy with selective double irradiation is clear.

Two-dimensional spectra were recorded on a Varian XL-200 spectrometer by transferring proton magnetization to naturally abundant carbon-13. The pulse sequence normally used for this experiment was only slightly modified, reducing the flip angle of the second pulse:

$$90^\circ(\text{H})-t_1-45^\circ(\text{H})90^\circ(\text{C}) \text{ Acquire } (t_2).$$

In practice 45° turns out to be a suitable compromise between the conflicting requirements for a small flip angle and good sensitivity. Lineshapes in both dimensions were improved by a combination of convolution difference (12) and Gaussian weighting of the time-domain signals.

The ABX spectrum of maleic anhydride provides a convenient test case for the method. The carbon-13 spin is X, and J_{AX} is the single-bond proton-carbon coupling (~ 190 Hz). Figure 1 shows the two-dimensional spectrum with the passive spins indicated in parentheses. Magnetization transferred from A to X shows two large square patterns displaced as indicated by the arrow marked (B). Since this has a positive slope, J_{AB} and J_{BX} have like signs. The long-range coupling J_{BX} is much smaller (~ 3 Hz), giving rise to incompletely resolved square patterns joined by the long arrow. This too has a positive slope, indicating that J_{AB} and J_{AX} also have like signs. Thus J_{HH} , J_{CH} , and J_{CCH} are all of the same sign in this molecule, presumably positive.

In more complicated systems of coupled spins, there may be more than one passive spin splitting the basic square pattern. The two-dimensional multiplets are correspondingly more complicated, but yield more information about relative signs so that cross-checks become possible.

One of the isotopomers of allyl alcohol illustrates such a case. Only the magnetization transferred from protons to a methylene carbon-13 nucleus is studied, and the spins are therefore labeled

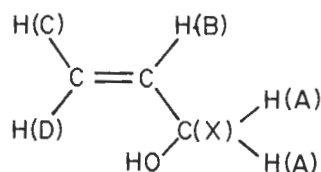


Figure 2 shows the resulting two-dimensional spectrum with passive spins indicated in parentheses. In general, transfer of magnetization between two given spins involves *three* passive spins and hence determines the relative signs of *three* pairs of spin coupling constants. In practice, slightly less information can be gleaned from this spectrum because J_{CD} is too small to give resolvable splittings on this frequency scale. Consider the two-dimensional spin multiplet at the bottom of Fig. 2, arising from magnetization transferred from proton B to X. The basic square pattern is split by coupling to A₂, C, and D, three nonequivalent spins

SIGNS^a AND J

Proton	Carbon
$J_{AB} = +4.9$	
$J_{AC} = -1.6$	
$J_{AD} = -2.0$	

^a Assuming t^b Sign not det

or groups of spins (A_2 similar displacements (indicated b that J_{AB} and J_{AX} have like have like signs. The other between A and X, C and X, signs, summarized in Table

A wealth of information therefore available by inspection by reducing the flip angle of This opens up the possible diagnostic tool.

This work was made possible by supported by a Stipend from the

1. D. F. EVANS AND J. P. MAH
2. R. FREEMAN AND D. H. WHI
3. R. FREEMAN AND W. A. ANI
4. S. ALEXANDER, *J. Chem. Ph*
5. J. JEENER, *Ampère Internatic*
6. W. P. AUE, E. BARTHOLDI, *J*
7. A. BAX AND R. FREEMAN, *J.*
8. A. A. MAUDSLEY AND R. R.
9. A. A. MAUDSLEY, L. MÜLLE
10. G. BODENHAUSEN AND R. FI
11. G. BODENHAUSEN AND P. H.
12. I. D. CAMPBELL, C. M. DOI

11, 172 (1973).

TABLE I
SIGNS^a AND APPROXIMATE MAGNITUDES (Hz) OF COUPLING
CONSTANTS IN ALLYL ALCOHOL

Proton-proton		Proton-carbon-13
$J_{AB} = +4.9$	$J_{BC} = +10.5$	$J_{AX} = +142$
$J_{AC} = -1.6$	$J_{BD} = +17.3$	$J_{BX} = +6$
$J_{AD} = -2.0$	$J_{CD} = \pm 2.1^b$	$J_{CX} = +13$
		$J_{DX} = +6$

^a Assuming the single-bond J_{CH} is positive.

^b Sign not determined because the splittings are not resolved.

or groups of spins (A_2 simply introduces a triplet structure). The corresponding displacements (indicated by the arrows) are all of positive slope, demonstrating that J_{AB} and J_{AX} have like signs, J_{BC} and J_{CX} have like signs, and J_{BD} and J_{DX} have like signs. The other multiplets in this spectrum, representing transfer between A and X, C and X, and D and X, provide further information on relative signs, summarized in Table I.

A wealth of information about the relative signs of spin coupling constants is therefore available by inspection of two-dimensional spectra of this kind, simply by reducing the flip angle of the mixing pulse in a magnetization transfer sequence. This opens up the possibility of a more widespread use of sign information as a diagnostic tool.

ACKNOWLEDGMENTS

This work was made possible by an equipment grant from the Science Research Council, and was supported by a Stipend from the Delft University Fund (A.B.).

REFERENCES

1. D. F. EVANS AND J. P. MAHER, *Proc. Chem. Soc. London*, 208 (1961).
2. R. FREEMAN AND D. H. WHIFFEN, *Mol. Phys.* **4**, 321 (1961).
3. R. FREEMAN AND W. A. ANDERSON, *J. Chem. Phys.* **37**, 2053 (1962).
4. S. ALEXANDER, *J. Chem. Phys.* **28**, 358 (1958).
5. J. JEENER, Ampère International Summer School, Basko Polje, Yugoslavia, 1971.
6. W. P. AUE, E. BARTHOLDI, AND R. R. ERNST, *J. Chem. Phys.* **64**, 2229 (1976).
7. A. BAX AND R. FREEMAN, *J. Magn. Reson.*, in press.
8. A. A. MAUDSLEY AND R. R. ERNST, *Chem. Phys. Lett.* **50**, 368 (1977).
9. A. A. MAUDSLEY, L. MÜLLER, AND R. R. ERNST, *J. Magn. Reson.* **28**, 463 (1977).
10. G. BODENHAUSEN AND R. FREEMAN, *J. Magn. Reson.* **28**, 471 (1977).
11. G. BODENHAUSEN AND P. H. BOLTON, *J. Magn. Reson.* **39**, 399 (1980).
12. I. D. CAMPBELL, C. M. DOBSON, R. J. P. WILLIAMS, AND A. V. XAVIER, *J. Magn. Reson.* **11**, 172 (1973).

ing of these components to allow passage through the pore into the cytosol.

A low pH trigger

The pH dependence of PA₆₈ membrane insertion suggests a molecular mechanism for triggering the release of the Domain 2 hairpin loop. Channel formation in artificial bilayers is greatly accelerated when the pH is lowered to values corresponding to the pK_as of histidine residues²⁰. Many of the histidine residues in the toxin are located in Domain 2. Protonation of some of these side-chains could be energetically unfavourable because of their location and the flipping out of the hairpin provides a mechanism for relieving the stress¹. There are, in fact, two crystal forms of the PA monomer obtained at different pH values of 7.5 and 6.0¹. The largest structural difference between them occurs at the tip of another loop in Domain 2 (residues 342–355) and includes three hydrophobic residues (Trp, Met and Leu). At pH 7.5, these residues are buried within the core of the domain but are exposed in the low pH form where the loop becomes disordered¹. This pH-dependent change may constitute another key event in the conversion of the heptamer from prepore to pore state.

Intriguingly, low pH appears to be a membrane insertion trigger for a num-

ber of protein toxins, although the way each toxin utilises a low pH environment appears different. In the case of colicins, low pH enhances the electrostatic attraction of one of its surfaces as it approaches the membrane^{17,21}. The low pH environment at the membrane surface facilitates the formation of a molten globule state²² and aids the insertion of amphipathic surfaces of the protein on application of an appropriate voltage^{6,17}. In diphtheria toxin, low pH is thought to act by favouring a monomeric form of the toxin²³ and by neutralizing carboxylate groups of a surface-exposed loop leading to the formation of a hydrophobic 'dagger' that triggers membrane insertion⁵.

Why a heptamer?

Protein complexes with sevenfold symmetry are rare in nature. Besides some chaperonin oligomers like GroEL²⁴, the only other complexes so far found with such symmetry are the apparently unrelated group of toxins including anthrax toxin protective antigen¹, α -haemolysin¹⁰ and aerolysin²⁵. There are a few common features between these toxins: they form mushroom-shaped oligomers with pores of similar sizes and are rich in β -sheet with no long stretches of hydrophobic residues. However, there is little, if any, sequence similarity between

them and the domain folds are very different. It is remarkable then they all form heptameric membrane pores. In the case of α -haemolysin, each monomer contributes two anti-parallel β -strands to the 14-stranded β -barrel and both PA and aerolysin are likely to be the same in this regard. However, it will be no surprise to find alternate β -barrel structures in membrane toxin pores in the future. Alternatives can be envisaged by analogy with the 16-stranded β -barrel structures of the bacterial porins^{7,8} and even larger β -sheet structures in the thiol-activated cytolysin family which can form oligomeric structures of more than 50 monomers²⁶.

The Ian Potter Foundation Protein Crystallography Laboratory, St. Vincent's Institute of Medical Research, 41 Victoria Parade, Fitzroy, Victoria 3065, Australia
mwp@rubens.its.unimelb.edu.au

- Petosa, C., Collier, R.J., Klimpel, K.R., Leppla, S.H. & Liddington, R.C. *Nature*, in the press.
- Protein Toxin Structure (ed Parker, M.W.) (R.G. Landes Company, Austin, Texas, 1996).
- Parker, M.W., Pattus, F., Tucker, A.D. & Tsernoglou, D. *Nature* **337**, 93–96 (1989).
- Li, J., Carroll, J. & Ellar, D.J. *Nature* **353**, 815–821 (1991).
- Choe, S. et al. *Nature* **357**, 216–222 (1992).
- Parker, M.W., Tucker, A.D., Tsernoglou, D. & Pattus, F. *Trends Biochem. Sci.* **15**, 126–129 (1990).
- Weiss, M.S. et al. *Science* **254**, 1627–1630 (1991).
- Cowan, S.W. et al. *Nature* **358**, 727–733 (1992).
- Parker, M.W. et al. *Nature* **367**, 292–295 (1994).
- Song, L. et al. *Science* **274**, 1859–1866 (1996).
- Leppla, S.H. in: *Bacterial Toxins and Virulence Factors in Disease* (eds Moss, J., Igilewski, B., Vaughan, M. & Tu, A.T.) 543–572 (Marcel Dekker, New York, 1995).
- Milne, J.C., Furlong, D., Hanna, P.C., Wall, J.S. & Collier, R.J. *J. Biol. Chem.* **269**, 20607–20612 (1994).
- London, E. *Mol. Microbiol.* **6**, 3277–3282 (1992).
- Little, S.F. et al. *Microbiology-UK* **142**, 707–715 (1996).
- Novak, J.M., Stein, M.-P., Little, S.F., Leppla, S.H. & Friedlander, A.M. *J. Biol. Chem.* **267**, 17186–17193 (1992).
- Singh, Y. et al. *J. Biol. Chem.* **266**, 15493–15497 (1991).
- Parker, M.W., Postma, J.P.M., Pattus, F., Tucker, A.D. & Tsernoglou, D. *J. Mol. Biol.* **224**, 639–657 (1992).
- Wiener, M., Freymann, D., Ghosh, P. & Stroud, R.M. *Nature* **385**, 461–464 (1997).
- Li, J., Koni, P.A. & Ellar, D.J. *J. Mol. Biol.* **257**, 129–152 (1996).
- Koehler, T.M. & Collier, R.J. *Mol. Microbiol.* **5**, 1501–1506 (1991).
- Zakharov, S.D., Heymann, J.B., Zhang, Y.-L. & Cramer, W.A. *Biophys. J.* **70**, 2774–2783 (1996).
- van der Goot, F.G., González-Mañas, J.M., Lakey, J.H. & Pattus, F. *Nature* **354**, 408–410 (1991).
- Eisenberg, D. et al. in: *Protein Toxin Structure* (ed Parker, M.W.) 25–47 (R.G. Landes Company, Austin, Texas, 1996).
- Saibil, H.R. et al. *Curr. Biol.* **3**, 265–273 (1993).
- Wilmsen, H.-U., Leonard, K.R., Tichelaar, W., Buckley, J.T. & Pattus, F. *EMBO J.* **11**, 2457–2463.
- Morgan, P.J. et al. *FEBS Lett.* **371**, 77–80 (1995).



Fig. 3 Ribbon representation of the anthrax toxin protective antigen heptamer. The view is from the top of the molecule down the seven-fold axis. The diameter of pore is, on average, ~35 Å. The domains are coloured as described in the legend of Fig. 2. (Figure reproduced from ref. 1 with kind permission).

Are proteins even floppier than we thought?

Ad Bax¹ and Nico Tjandra²

With ever stronger magnetic fields, magnetic alignment of proteins and nucleic acids with the magnetic field can now be observed. In such magnetically aligned systems, dipolar couplings no longer average to zero and the residual splittings contain unique information on molecular conformation and possibly mobility.

Structure determination by solution NMR so far has been based entirely on the very local information contained in NOEs, J -couplings and chemical shifts¹⁻⁴. NOEs provide the all-important interproton distance information, but for a variety of technical reasons these are in practice only interpreted as semi-quantitative measures for the time-averaged interproton distance. Three-bond J -couplings intrinsically are highly accurate reporters on the intervening dihedral angle⁵, but their measurement is often fraught with difficulty, particularly in larger systems where the natural resonance line width exceeds that of the small J -couplings. Chemical shifts, in contrast, can be easily measured with high accuracy, and are exquisitely sensitive to local geometry⁶. Unfortunately, at present our knowledge of the various factors determining chemical shifts, in particular those of ¹³C and ¹⁵N, remains incomplete. Therefore, these shifts too can only be interpreted as a qualitative indicator for backbone geometry and very local packing. Thus, it may be considered remarkable, and perhaps surprising, that macromolecular structures can be determined at all by NMR spectroscopy. The reason why the method works for globular structures is that 'long range' NOEs, corresponding to short interproton distances between residues far apart in the polymer sequence, are conformationally highly restrictive. However, it is clear that the NMR method has been weak at determining structures of molecules that lack such long-range constraints. For example, it is difficult to distinguish straight double-stranded DNA from slightly curved DNA on the basis of NMR data. Similarly, the method has been ineffective at deter-

mining relative positions of protein domains in cases where few interdomain NOEs can be identified.

A common assumption made in solution NMR is that, over time, a given protein will sample all orientations with respect to the static magnetic field with equal probability, and consequently that all dipolar interactions average to zero. In the absence of such averaging, that is, in

exhibit a minute residual splitting, which scales with the square of the magnetic field⁷⁻⁹. More recently, Prestegard and co-workers demonstrated that such residual dipolar couplings, on the order of a few Hz, can also be observed in paramagnetic cyanometmyoglobin¹⁰, and we measured such splittings in human ubiquitin¹¹, a diamagnetic protein with a ~10-fold smaller susceptibility anisotropy and proportionately smaller dipolar couplings. These dipolar couplings carry information on the orientation of a bond vector relative to the protein's magnetic susceptibility tensor, that is, they can orient bond vectors all relative to the same frame, regardless of their location in the molecule. This distinguishes these constraints from all other constraints used during NMR structure calculation, such as NOEs, J -couplings and chemical shifts, which are strictly local in nature. By their ability to define such long range order, dipolar couplings offer a potential cure to one of the principal remaining weaknesses of the NMR structure determination method.

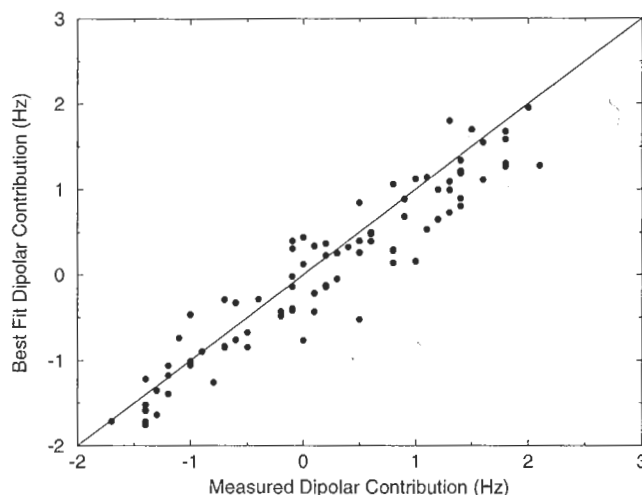


Fig. 1 Plot of the myoglobin dipolar couplings, kindly provided to us by Tolman et al¹², versus those predicted by a 'best-fit' magnetic susceptibility tensor with $\Delta\chi = 1069 \text{ V}\cdot\text{V}\cdot\text{mol}^{-1}$, $\delta\chi = -415 \text{ V}\cdot\text{V}\cdot\text{mol}^{-1}$ and $\alpha = -19^\circ$, $\beta = -18^\circ$, $\gamma = 73^\circ$.

the solid state, a dipolar interaction between atoms I and S is proportionate to $\gamma_I \gamma_S r_{IS}^{-3}$, where γ is the magnetogyric ratio and r_{IS} the internuclear distance. This interaction results in a splitting in the I-spin and S-spin spectra proportionate to $\gamma_I \gamma_S r_{IS}^{-3} (3\cos^2\theta - 1)$, where θ is the angle between the I-S vector and the direction of the static magnetic field. For directly bonded pairs of atoms such as N-H or C-H pairs, where the internuclear distance is known, the dipolar interaction therefore provides a measure for the angle θ . Many years ago, Bothner-By and co-workers demonstrated that in solution the dipolar couplings in molecules with a significantly anisotropic susceptibility tensor no longer average to exactly zero but

Determination of the susceptibility tensor

The magnetic susceptibility of macromolecules is generally assumed to correspond to the sum of the susceptibility tensors of its components. Whereas peptide groups contribute small amounts, contributions from aromatic rings are about an order of magnitude larger. The susceptibility tensor of paramagnetic sites or certain prosthetic groups such as haems is yet another order of magnitude larger. Therefore, although all proteins in principle have a non-zero magnetic susceptibility tensor, paramagnetic proteins frequently have considerably larger susceptibility anisotropies than diamagnetic proteins. If

the structure of a protein is known, its susceptibility tensor can be predicted from the sum of its individual components. Alternatively, the susceptibility tensor can be determined experimentally by searching for the tensor that minimizes the difference between the individually measured dipolar couplings and those predicted by the susceptibility tensor, using the known relative positions of the dipolar coupled pairs of atoms, I and S¹¹. This amounts to a three- or five-dimensional search problem in the case of an axially symmetric or a fully asymmetric susceptibility tensor, which can readily be solved provided the number of dipolar couplings measured is much greater than this number of unknowns¹¹.

If the protein structure were static, that is, in the absence of internal motions, one would expect good agreement between the calculated and experimentally derived magnetic susceptibility tensors, provided the susceptibilities of the individual groups are known accurately and the protein is fully monomeric. Small amplitude internal motions about the average positions, however, will scale down the dipolar couplings by a factor that corresponds to the generalized order parameter S^{11-13} . Except for flexible loop regions, extensive measurement of ¹⁵N relaxation times indicates that, at least for ¹⁵N-¹H pairs, S^2 values are relatively uniform and have values of $S^2 = 0.85 \pm 0.04$, or $S = 0.92 \pm 0.02$ (ref. 14). However, it should also be emphasized that ¹⁵N relaxation measurements, and thereby S^2 values, only reflect motions faster than the overall tumbling of the protein, that is, faster than ~10 ns. Dipolar couplings measured for cyanometmyoglobin by Tolman *et al.*¹² are about 27% smaller than values predicted by its crystal structures; these authors interpret this difference as evidence for very low order parameters, that is, very large amplitude motions.

Floppy myoglobin?

The two major contributions to the magnetic susceptibility tensor of myoglobin have opposite sign and stem from the paramagnetism of the metal and the diamagnetism of the haem. The paramagnetic term has been determined by LaMar and co-workers¹⁶ on the basis of paramagnetic shifts of protons close to the metal centre, assuming the myoglobin structure to be static and identical to the crystal structure. The diamagnetic susceptibilities of several porphyrins have been measured⁸ and their values are expected to be representative for the myoglobin

haem. As mentioned above, fitting of the N-H dipolar couplings measured by Tolman *et al.*¹² to either the X-ray or neutron diffraction crystal structure of cyanometmyoglobin yields a susceptibility tensor which is 27% smaller than the one predicted on the basis of the sum of the paramagnetic and diamagnetic components. Systematic errors in the measurement of the dipolar couplings presumably can be excluded because very similar values were measured with different pulse schemes. Tolman *et al.* interpret the difference between the predicted and measured dipolar couplings as evidence for large amplitude dynamics. However, as amide hydrogen exchange rates are slow, hydrogen bonds must remain intact. This therefore suggests that it is not the individual amide N-H bond vectors that are undergoing the large amplitude angular excursions, but that myoglobin's α -helices move as intact units relative to one another. Indeed, this conclusion finds some support in the so-called 'essential dynamics' description of protein dynamics by the Berendsen group¹⁷. There are also numerous sources of other experimental evidence that such motions indeed can occur: experimentally observed hydrogen exchange requires local unfolding and solvent access, even in the core of the protein¹⁸; access of small ligands into the core of a protein is relatively fast¹⁹; rapid flipping (typically on a ms time scale) of the aromatic Phe and Tyr rings requires motions by several Ångströms of nearby groups²⁰; and even the haem itself can flip up-side down, although the latter is a very slow process²¹.

The difference in the conclusions by Tolman *et al.*¹² relative to these other experimental findings is that the large amplitude deviations from the average structure do not occur just occasionally, but are present all the time: on average, the axis orientations of several of myoglobin's helices differs by 25° or more from their time-averaged positions. As ¹⁵N relaxation times do not show any evidence for such large amplitude motions, they must occur on a time scale slower than that of rotational diffusion (~10 ns). However, they also must be faster than milliseconds because slower motions would result in very extensive line-broadening in the NMR spectrum.

On the other hand, there are also strong experimental arguments against such an extremely dynamic 'jello-like' myoglobin model. First, if myoglobin indeed were as dynamic as concluded by Tolman *et al.*, the measurement of the paramagnetic

term of the susceptibility tensor by LaMar and co-workers¹⁶ on which Tolman's conclusions are based, would be in error as the LaMar study assumed a static myoglobin model. Second, the very good correlation between experimentally observed ring current shifts, which are exquisitely sensitive to small local changes in structure, and those predicted by a static crystal structure²² suggests that the structure must remain close to that observed in the crystalline state for a large fraction of time. Third, because in the jello-myoglobin model interhelical proton pairs would only be present for a very short fraction of the time, one would expect intra-helical NOEs to be much stronger than interhelical NOEs. Fourth, one would expect numerous weak interhelical NOEs that cannot be satisfied simultaneously, reflecting the distribution of interhelical NOE contacts a given proton samples over time. Although some evidence for the latter exists in a limited number of cases, usually they can be explained by small local rearrangements.

The conclusion of large amplitude collective motions in myoglobin is based on the difference between the measured and the predicted dipolar couplings in myoglobin. This conclusion conflicts with the widely held view of proteins as having rather well-defined backbones, with very rapid (sub-ns), relatively small amplitude oscillations about this average. The large amplitude motions invoked in the Tolman study would require most of the interactions which stabilize the protein's tertiary structure to be present for only a small fraction of the time. It is important to note, however, that Tolman's dipolar couplings themselves are in reasonable agreement with the static crystal structure, provided the magnitude and orientation of the magnetic susceptibility tensor are allowed to float (Fig. 1). This latter approach yields a $\Delta\chi$ which is about 27% smaller and an orientation of the $\Delta\chi$ symmetry axis which differs by ~9° from the predicted one. The answer to the question of whether the collective, intermediate time scale motions in myoglobin are real or not hinges on how reasonable a 27% difference is between the best-fit and the tensor predicted for static myoglobin. This amounts to a difference of 19% relative to the tensor predicted for myoglobin with $S^2 = 0.85$. Tolman *et al.* do not believe such a large difference is credible. In our opinion, however, it is conceivable that there are other factors, not accounted for in the Tolman study, which could influence the magnetic susceptibility ten-

news and views

sor. For example, very weak intermolecular interaction at the high protein concentration used in the myoglobin study could alter the degree of magnetic alignment. It also would be interesting to measure the dipolar couplings in diamagnetic carbon-monoxymyoglobin, which would permit separation of the diamagnetic and paramagnetic contributions, and could rule out significant errors in the $\Delta\chi$ used for the haem.

Ubiquitin is the only other protein for which the predicted and experimentally determined magnetic susceptibility tensors have been compared¹¹. Two sets of measurements, initially at 360 and 600 MHz¹¹ and subsequently repeated at 360 and 750 MHz, show quite good agreement with one another and yield magnetic susceptibility anisotropy tensors that are only slightly smaller than predicted from the sum of the group susceptibilities. This suggests that large amplitude motions are not present in ubiquitin.

Because dipolar couplings are relatively insensitive to motion (they scale with S and not with S^2), Tolman *et al.* needed to

invoke rather extreme degrees of mobility to explain the discrepancy between observed and predicted dipolar couplings. If the susceptibility tensor is derived from the dipolar couplings themselves, no large amplitude dynamics are needed to explain the data and good agreement with the myoglobin crystal structure is obtained. In our opinion, therefore, because dipolar couplings are exquisitely sensitive to structure but only weakly to dynamics, they hold most promise for structure determination¹⁰, not for the study of dynamics.

¹Laboratory of Chemical Physics, Building 5, National Institute of Diabetes and Digestive and Kidney Diseases and ²Laboratory of Biophysical Chemistry, Building 3, National Heart, Lung, and Blood Institute, National Institutes of Health, Bethesda, Maryland 20892, USA Email: bax@nih.gov

1. Wüthrich, K. *NMR of Proteins and Nucleic Acids* (Wiley, New York 1986).
2. Case, D. E., Dyson, J. & Wright, P. *Methods. Enzymol.* **239**, 392–415 (1994).
3. Gronenborn, A. M. & Clore, G. M. *CRC Crit. Rev. Biochem. Mol. Biol.* **30**, 351–385 (1995).

4. Cavanagh, J., Fairbrother, W. J., Palmer III, A. G. & Skelton, N. J. *Protein NMR Spectroscopy, Principles and Practice* (Academic Press, San Diego 1996).
5. Wang, A. C. & Bax, A. *J. Am. Chem. Soc.* **118**, 2483–2494 (1996).
6. Osapay, K. & Case, D. A. *J. Am. Chem. Soc.* **113**, 9346–9444 (1996).
7. Gayathra, C., Bothner-By, A. A., van Zijl, P. C. M. & MacLean, C. *Chem. Phys. Lett.* **87**, 192–196 (1982).
8. Bothner-By, A. A. *et al. Magn. Reson. Chem.* **23**, 935–938 (1985).
9. Bothner-By, A. A. in *Encyclopedia of Nuclear Magnetic Resonance* (eds Grant, D. M. & Harris, R. K.) 2932–2938 (Wiley, Chichester, 1995).
10. Tolman, J. R., Flanagan, J. M., Kennedy, M. A. & Prestegard, J. H. *Proc. Natl. Acad. Sci. USA* **92**, 9279–9283 (1995).
11. Tjandra, N., Grzesiek, S. & Bax, A. *J. Am. Chem. Soc.* **118**, 6264–6272 (1996).
12. Tolman, J. R., Flanagan, J. M., Kennedy, M. A. & Prestegard, J. H. *Nature Struct. Biol.* **4**, 292–297 (1997).
13. Lipari, G. & Szabo, A. *J. Am. Chem. Soc.* **104**, 4546–4558 (1982).
14. Kay, L. E., Torchia, D. A. & Bax, A. *Biochemistry* **28**, 8972–8979 (1989).
15. Vijay-Kumar, S., Bugg, C. E. & Cook, W. J. *J. Mol. Biol.* **194**, 531–544 (1987).
16. Rajarathnam, K., LaMar, G. N., Chiu, M. L. & Sligar, S. G. *J. Am. Chem. Soc.* **114**, 9048–9058 (1992).
17. Amadei, A., Linssen, A. B. M., & Berendsen, H. J. C. *Proteins* **17**, 412–425 (1993).
18. Englander, S. W. & Kallenbach, N. R. *Q. Rev. Biophys.* **16**, 521–655 (1984).
19. Feher, V. A., Baldwin, E. P. & Dahlquist, F. W. *Nature Struct. Biol.* **3**, 516–521 (1996).
20. Wagner, G. *Q. Rev. Biophys.* **16**, 1–57 (1983).
21. Jue, T., Krishnamoorti, R. & LaMar, G. N. *J. Am. Chem. Soc.* **105**, 5701–5703 (1983).
22. Osapay, K., Theriault, Y., Wright, P. E. & Case, D. A. *J. Mol. Biol.* **244**, 183–197 (1994).

How Src exercises self-restraint

Jack T. Nguyen¹ and Wendell A. Lim^{1–3}

Two recent landmark structures of Src family kinases reveal how a sensitive conformational switch can be built with SH2 and SH3 domains.

The c-Src kinase and its family of homologues have long been known to function as molecular switches, playing a critical role regulating cell growth and differentiation^{1,2}. In the oncogene v-Src this switch is broken; mutations result in a constitutively active kinase, and consequently transformation. The precise mechanism by which this switch works has remained elusive after many years of research, although it has been clear for some time that the well-studied Src

Homology 2 and 3 (SH2 and SH3) domains play a central role in the process. Sicheri *et al.* and Xu *et al.* have now solved the crystal structures of the nearly intact Hck and Src kinases, respectively, in their repressed states^{3,4}. These structures reveal a remarkable, conserved network of intramolecular interactions involving the SH2 and SH3 domains, which together appear to stabilize the inactive conformation of the kinase. The structures show that Src

kinase repression is built upon subtle layers of interdependent interactions which could be disrupted by multiple activating inputs.

Src Family Kinases and Src Homology Domains

To date, nine members of the Src kinase family have been identified: Src, Fyn, Yes, Fgr, Lyn, Hck, Lck, Blk, and Yrk^{1,2}. While the expression of Src is ubiquitous, expression of other family mem-

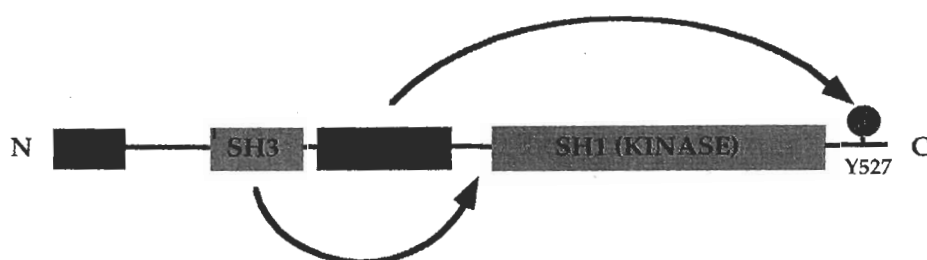


Fig. 1 Domain organization of Src-family kinases. The SH4 domain contains a myristoylation site and serves to anchor the protein to the cell membrane. SH2 and SH3 domains mediate protein–protein complexes. Phosphorylation of Tyr 527 in the C terminus by Csk is necessary for the regulation of kinase activity. Arrows represent intramolecular interactions observed in the repressed state crystal structures of Src and Hck.